

Predicting and Optimizing Ergonomics in Physical Human-Robot Cooperation Tasks

van der Spaa, Linda ; Gienger, Michael; Bates, Tamas; Kober, Jens

DOI

[10.1109/ICRA40945.2020.9197296](https://doi.org/10.1109/ICRA40945.2020.9197296)

Publication date

2020

Document Version

Accepted author manuscript

Published in

Proceedings of the IEEE International Conference on Robotics and Automation, ICRA 2020

Citation (APA)

van der Spaa, L., Gienger, M., Bates, T., & Kober, J. (2020). Predicting and Optimizing Ergonomics in Physical Human-Robot Cooperation Tasks. In *Proceedings of the IEEE International Conference on Robotics and Automation, ICRA 2020* (pp. 1799-1805). IEEE.
<https://doi.org/10.1109/ICRA40945.2020.9197296>

Important note

To cite this publication, please use the final published version (if applicable).
Please check the document version above.

Copyright

Other than for strictly personal use, it is not permitted to download, forward or distribute the text or part of it, without the consent of the author(s) and/or copyright holder(s), unless the work is under an open content license such as Creative Commons.

Takedown policy

Please contact us and provide details if you believe this document breaches copyrights.
We will remove access to the work immediately and investigate your claim.

Predicting and Optimizing Ergonomics in Physical Human-Robot Cooperation Tasks

Linda van der Spaa^{1,2}, Michael Gienger², Tamas Bates^{1,2}, Jens Kober¹

Abstract—This paper presents a method to incorporate ergonomics into the optimization of action sequences for bimanual human-robot cooperation tasks with continuous physical interaction. Our first contribution is a novel computational model of the human that allows prediction of an ergonomics assessment corresponding to each step in a task. The model is learned from human motion capture data in order to predict the human pose as realistically as possible. The second contribution is a combination of this prediction model with an informed graph search algorithm, which allows computation of human-robot cooperative plans with improved ergonomics according to the incorporated method for ergonomic assessment. The concepts have been evaluated in simulation and in a small user study in which the subjects manipulate a large object with a 32 DoF bimanual mobile robot as partner. For all subjects, the ergonomic-enhanced planner shows their reduced ergonomic cost compared to a baseline planner.

I. INTRODUCTION

Industrial robots have begun to leave their cages, but are not yet anywhere near the point where they can cooperate with humans at an equal level. Through physical assistance and cooperation, robots have a large potential to make human lives easier and prevent musculoskeletal disorders (MSDs). However, physical Human-Robot Interaction (pHRI) is still largely restricted to handling, lifting, and positioning scenarios in which robots do not have the autonomy to plan their provided assistance themselves [1].

For example, consider the case of moving a large object that is too heavy or bulky to be safely and comfortably manipulated by one person. In such cases a cooperative robot providing physical assistance could take most of the weight, or at least support the object in a way that allows the human to remain in a comfortable, ergonomic posture. Non-ergonomic poses are very high on the list of causes of work-related MSDs [2], closely followed by heavy physical work and lifting. Product lifecycle management software, like Siemens Jack [3], is used in industry to optimize the ergonomics of products or processes, including collaborative robot arms [4], in the design phase. However, such tools are typically useful for static environments or processes which do not involve any on-the-fly customization or adaptation to specific users. Incorporating human ergonomics measurements in the decision-making process of cooperative robots at run-time has the potential to improve the long-term impact

¹Delft University of Technology, Mekelweg 2, 2628CD The Netherlands {l.f.vanderspaa, j.kober}@tudelft.nl, tamas.bates@tum.de

²Honda Research Institute Europe, Offenbach, Germany michael.gienger@honda-ri.de

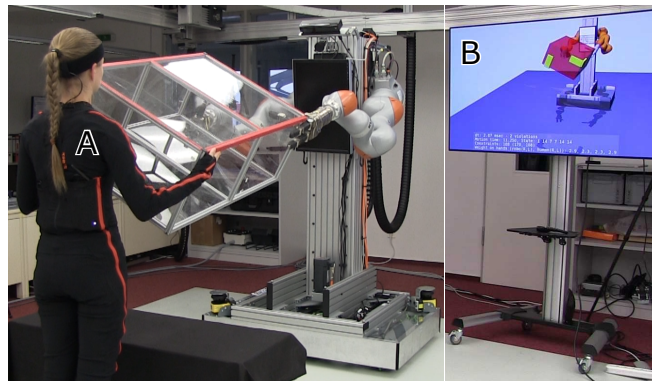


Fig. 1. Robot test setup of the human-robot cooperative planner. A: The human partner wears a full-body motion capture suit (for validation). B: The screen displays the cooperative plan for both partners.

on workers even when the task and physical environment may be highly dynamic or unknown in advance.

In this paper, ergonomic optimization is applied to the task of manipulating a large object, which requires continuous interaction between the robot and the human partner. The presented ergonomic planner extends the sequential planner of [5] to select a sequence of states which is ergonomically optimal for the human partner. The new planner is applied to the task of rotating large objects (Fig. 1).

The contribution of this paper is twofold: 1) We develop a model that predicts the ergonomics of a human within a human-robot collaborative task (Sec. IV). 2) This ergonomics predictor is integrated in sequential task planning (Sec. V), resulting in a joint plan for the human and robot movements optimized for human ergonomics. Subsequently, Sec. VI explains how this method is applied to our test case. The presented ergonomic planner is compared to a baseline planner which optimizes solely for a minimum time solution, without additionally optimizing for the partner ergonomics. The simulation results and user study evaluation are presented in Sec. VII. Our findings are concluded and discussed in Sec. VIII. But first, related work is discussed in Sec. II and a system overview given in Sec. III.

II. RELATED WORK

Literature shows various research on physical human-robot cooperation (pHRC), improving ergonomic working conditions, and some steps towards integrating the two.

A. Physical Human-Robot Cooperation

An important area of pHRC research focuses on a human and robot jointly manipulating a single tool [6]–[8]. These

problems require a form of impedance control, which allows stiffnesses to be varied to achieve improved trajectory tracking while decreasing the human task effort. This form of co-manipulation has been extended to cooperative carrying of objects, still using impedance control to manage the interaction forces between the robot and human [9], [10]. Instead of using the position of the manipulator or manipulated object for impedance control, EMG signals have been successfully used as an input “intention estimate” for controlling cooperative object manipulation [11], [12].

A different form of cooperative physical interaction is observed in object hand overs. Much research in this area has focused on predicting where the human will move his/her hand [13] or, incorporating knowledge of a task model, classifying the intended (next) action [14], [15].

More complex, sequential, tasks that require regripping during co-manipulation of objects have been addressed in [16], in which a planner was developed for dyadic collaborative manipulation, which includes a model of the human as an active agent who shares the task objective.

B. Optimizing Ergonomics in pHRC

Ergonomic optimization has made a recent appearance in the field of pHRC. So far two trends have been observed.

The first trend is the task of holding a workpiece in the optimal position in space while a human works on it. For example, in tasks like drilling in which a human applies a tool to an object, the position of the object held by a robot has been ergonomically optimized to minimize joint torques [17], [18], muscular effort [19] or the RULA score [20], [21].

The second trend, in the domain of sequential tasks, is in optimizing the ergonomics for short moments of interaction during the handover of objects [22]. In these cases the human pose only depends on the robot in the brief instants of the handover, and each handover pose is independent of the previous ones.

C. Ergonomic Measures

Extensive bio-mechanical models exist (e.g. [23]) which can be used to simulate human bodies to extract information that cannot be directly obtained from sensors. However, the complexity of full musculoskeletal models makes them computationally expensive to use. In [19] a full musculoskeletal model is used to train a low dimensional latent variable model, which is then used for minimizing muscle activation in a bimanual drilling task. In [17], [18], a weighted sum of joint torques has been used as an ergonomic measure, in which the joint torques were obtained from the full-body pose combined with the estimated respectively measured center of pressure.

Many methods in practical use are based on tables and checklists [24] designed for manual evaluation of tasks by an ergonomics expert. A generally accepted and popular method for full-body evaluation, verified by ergonomic experts and easy to automate, is the Rapid Entire Body Assessment (REBA) [25] (which is the full-body extension of RULA [21]). REBA requires measurement of the full-body pose and estimation of the external forces acting on the body.

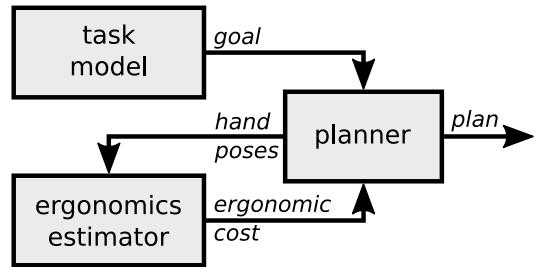


Fig. 2. System overview: The task model provides a goal. In order to reach this goal, the planner proposes sequences of hand poses. An ergonomics estimator is developed to evaluate the ergonomic cost of these hand poses, such that minimizing this cost results in an ergonomic task solution.

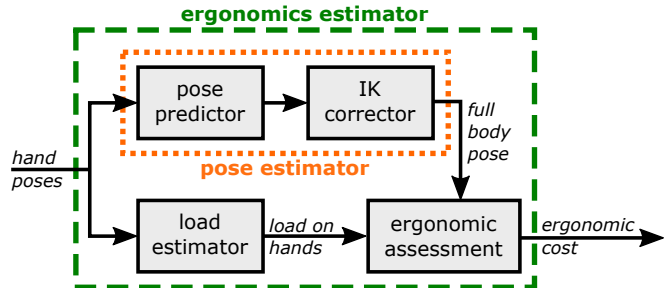


Fig. 3. Predicting the ergonomic cost from hand poses.

III. SYSTEM OVERVIEW

The focus of this paper is the design of a method for ergonomic planning of tasks in which both human and robot need to coordinate their movements to satisfy the constraints of the task (e.g. do not drop the object). To this end, we developed a method to estimate the ergonomic cost based on a prediction model of the human’s pose and loads (Sec. IV). This predicted ergonomic cost is then incorporated in a sequential planner (Sec. V). A schematic overview of the two components and their interaction is given in Fig. 2.

IV. ERGONOMICS PREDICTOR

In order to estimate the ergonomics (Sec. IV-A) of the hand poses, we need to predict the postures the human will use to obtain these hand poses, as well as the load that will act on the human in these postures (Fig. 3). For predicting the posture, we employ a learned pose predictor combined with an inverse kinematics correction to estimate the full-body pose of the human based on his/her hand poses (Sec. IV-B). The load is estimated based on the hand poses of the human and the robot, combined with the physical properties of the manipulated object (Sec. IV-C).

A. Ergonomic Assessment

In this paper, we chose REBA [25] as the ergonomics assessment method. By using a standardized ergonomics metric, we expect that our results will be compatible with existing ergonomics practices. Even so, the metric is easily replaceable by any other measure derivable from pose and load information.

REBA applies a set of tables to evaluate the human posture from joint angles augmented with some additional

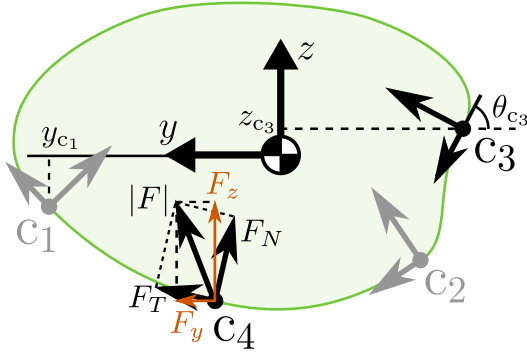


Fig. 4. An object supported at four points, by: c_1 : robot right, c_2 : robot left, c_3 : human right, and c_4 : human left hand. At each contact point, the total force F is the vector sum of the normal force F_N , acting in direction θ , and a tangential force F_T , which can be decomposed into vectors pointing in y and z direction. The x direction is defined from the human to the robot.

information, e.g., external loads (Sec. IV-C) or whether the human is standing on one leg. The resulting score ranges from 1 (negligible risk) to a maximum of 12 (high risk: 8-10, very high risk: 11+).

The original REBA assessment considers only one active arm. For the bimanual tasks we are considering, we evaluate the arm that is the least ergonomic in order to compute the worst-case REBA score. The full-body pose score is integrated over time to evaluate and compare plans.

B. Full-Body Pose Estimator

For the ergonomic assessment, we need to infer a full-body pose given the hand poses. Mapping hand poses to a full-body pose is a redundant problem, which we chose to solve in the following two steps:

1) *Learned Pose Predictor From Data*: maps the two human hand poses to the human's full-body pose by means of supervised learning. Given that the training data does not always cover the whole input space, there might be small errors in these predictions.

Since the mapping from hand poses to full-body poses is not unique, we record humans to get full-body poses that are typically employed. The datasets contain full-body joint angles (59 degrees of freedom) and a corresponding forward kinematic model. We learn a nearest neighbor (NN) map and an LWPR model [26]. The models are trained on the hand poses obtained by the forward kinematics model from the recorded poses. Evaluation and selection of the models is discussed in Sec. VI.

In any case, the hand positions and orientations of the estimated full-body pose will not exactly match the target. This is corrected in the next step:

2) *Inverse Kinematic (IK) Pose Correction*: makes the hands of the full-body pose match the hand poses.

The IK pose correction step will correct the pose to comply with the human hand poses. Additional constraints are applied to align the feet with the ground plane, and to keep the overall center of mass balanced. See [27] for details.

C. Hand Load Estimator

The load on each human hand is estimated based on the hand poses of the human and robot as well as physical properties (such as the mass, geometry, and friction parameters) of the manipulated object. To do so, we solve the following optimization problem: each of the hands is allowed to exert a normal force F_N and a tangential force F_T (as depicted in Fig 4). Static balance is assumed at all times. Two reasons support this assumption: all (allowed robot) motions are slow, and the planner only considers configurations in which it should be possible to halt the plan, for example, to wait for a confirmation to continue.

The optimization criterion is the square of the resultant forces summed over all hands in contact, which expresses the desire to hold the object as lightly as possible. Given which hands are in contact with the object, Eq. (1) describes the optimization problem:

$$\min \sum_{i=\text{hands.in.contact}} (F_{N,i}^2 + F_{T,i}^2) \quad (1)$$

subject to the following bounds for each of the hands:

$$-\sqrt{F_{\text{maxPull},i}^2 - F_{\text{maxT},i}^2} \leq F_{N,i} \leq \sqrt{F_{\text{maxPush},i}^2 - F_{\text{maxT},i}^2} \quad (1a)$$

$$-F_{\text{maxT},i} \leq F_{T,i} \leq F_{\text{maxT},i} \quad (1b)$$

and the static balance constraints,

$$\sum_i F_{x,i} = 0, \quad \sum_i F_{y,i} = 0, \quad \sum_i F_{z,i} = mg, \quad (1c)$$

$$\sum_i M_{x,i} = 0, \quad \sum_i M_{y,i} = 0, \quad \sum_i M_{z,i} = 0, \quad (1d)$$

where $F_{\text{maxPull},i}$, $F_{\text{maxPush},i}$, and $F_{\text{maxT},i}$ are the maximum pulling, pushing, and tangential forces for each of the (robot and human) hands in contact. Gravity g is acting on the object's mass m in the negative z -direction (Fig. 4). The solution of this optimization problem is the set of minimum hand forces required to hold the object in static balance.

V. ERGONOMIC PLANNER

For planning, the general planning architecture of [5] has been extended to include the ergonomic cost of the human partner. Given some goal state provided by the task model (Fig. 2), the state space is searched for a sequence of states to reach the goal with minimum cost. This plan can be converted to smooth motion trajectories for the robot's hands, and through full-body IK, motor commands for the robot hardware can be computed. For further details, the reader is referred to [5].

Given an object of known size and weight, the tasks we consider are formulated in terms of the desired position and orientation (pose) of the object. In order to plan how best to cooperatively manipulate the object to achieve this goal, the underlying state description comprises the object pose as well as the contact locations for robot and human hands. Fig. 5 depicts the discrete state description for the box object used in our study. However, the face of the object can have an arbitrary shape. Possible contact locations are defined evenly distributed around the graspable surface of the object, with

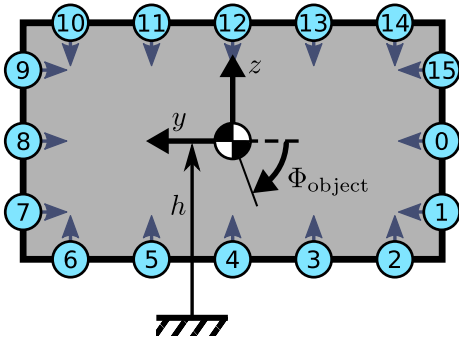


Fig. 5. State description. The numbers in the circles enumerate the contact locations on one side of the object. Discretized height h (from ground) and angle Φ_{object} define the position and orientation of the object.

the hand normal vector always perpendicular to the object surface. In this way, the index of the contact location suffices to describe the position and orientation of each hand.

An A^* graph search is applied to find a state sequence which is optimal with respect to some cost criterion. Costs accumulate as the planner explores possible next states in the sequence and each transition from one state to the next has an associated cost. In [5], this transition cost was proportional to the time the robot needed for the transition.

In the ergonomic planner, the transition cost is extended by the predicted ergonomic cost of the human partner. With the method presented in Sec. IV, the REBA score can be computed for each of the states proposed by the planner. It is assumed that subsequent states are close enough, and the change between them slow enough, that the properties (such as pose and load) during the transition between the states can be estimated sufficiently by linear interpolation between the enclosing states. Currently, we assume each state transition to have a fixed duration. Therefore, we assume the ergonomics of the transitions can be compared by taking the average REBA score of the enclosing states.

The human ergonomic cost term is scaled to dominate the previously described robot cost by one order of magnitude. When different possible successor states have the same cost, the planner is biased towards selecting the next state which requires the least movement. While not exploited in the experiments, it should be stated that our planning architecture allows for specifying an upper bound on the permissible ergonomic cost. This can easily be incorporated into the employed planner by rejecting states with an ergonomic cost larger than a given limit.

VI. EVALUATION SCENARIO

In this paper, the method is applied to a cooperative object rotation task in which the object is held on one side by the robot and on the other side by a human. A proof-of-concept user study with four subjects was conducted with a rectangular box of dimensions $0.63 \times 0.36 \times 1.0$ m, weighing 10 kg (Fig. 1). The box is rotated in the 2D plane around the axis pointing from the human to the robot. Translation is only allowed in the vertical direction, as specified by h . The state space is defined as in Fig. 5, with angles

TABLE I

MODEL ESTIMATION ERRORS, MEAN \pm STD, FOR THE NN AND LWPR PREDICTORS WITH DIFFERENT ANGLE WEIGHT FACTORS.

Angle weight factor		0.0	0.1	0.2	0.3	0.4	0.5
NN	$ \vec{x} $ in cm	13 \pm 8.2	13 \pm 8.2	13 \pm 7.5	14 \pm 7.6	15 \pm 8.3	15 \pm 8.7
	\angle in deg	30 \pm 34	21 \pm 18	17 \pm 10	15 \pm 9.6	14 \pm 8.9	14 \pm 8.5
LWPR	$ \vec{x} $ in cm	15 \pm 10	14 \pm 9.1	16 \pm 10	15 \pm 9.3	17 \pm 8.7	14 \pm 8.3
	\angle in deg	39 \pm 35	36 \pm 31	30 \pm 37	22 \pm 26	26 \pm 34	16 \pm 22

$\Phi_{\text{object}} \in \{0^\circ, \Delta\Phi, \dots, 360^\circ - \Delta\Phi\}$, $\Delta\Phi = 30^\circ$ and heights $h \in \{0.5, 0.5 + \Delta h, \dots, 2.0\}$, $\Delta h = 0.1$ in meters. This section presents the relevant implementation details to the simulation tests and user study discussed in Sec. VII.

A. Pose Estimation

Each participant was equipped with a motion capture suit for data collection, and was asked to move and rotate the box with a human partner. A corresponding dataset of about 1.5 min with a sampling time of 4 ms was recorded. Participants were guided to move the box through a large range of positions in the overall task space. The obtained dataset was used to train a subject-specific pose predictor which, after IK correction, provides a pose estimate that reflects the respective participant's personal pose behavior. The smaller the IK correction can be kept, the more human-like the predicted poses will be, and the more personal behavior is captured.

The pose predictor is trained to estimate the full-body pose from hand positions and orientations. A weight factor scales the importance of the orientations with respect to the positions. One set of training data (18k samples) was used to train the NN and LWPR predictors with different angle weight factors. The models were evaluated with a different dataset (25k samples) containing similar poses of the same person. The results are shown in Table I.

In general, the NN prediction results in a lower mean error and smaller standard deviation compared to the LWPR. The differences are small for the position precision, but the NN predictor performs much better when it comes to predicting the correct angles of the hands. An angle weight factor of 0.3 was chosen for the subsequent experiments, trading off position and orientation.

The body pose estimation, especially the IK correction step, is too computationally expensive for the planner to run on every state evaluation. As the set of states considered during planning is discrete and finite, we generate a table which contains the full-body pose stored for every set of unique human hand states and object heights. Then, during search, only this table needs to be evaluated in order to obtain the pose for ergonomic evaluation.

B. Load Estimation

Currently, we disallow grasping (and hence pulling). For the robot this will always be the case, as it is not able to grasp the objects. The people in the study were instructed not to grasp, only support, the object. Thus, all forces in x direction,

TABLE II

PARAMETERS AND CONSTRAINT VALUES FOR THE LOAD ESTIMATION

maximum human pulling force	$F_{h,maxPull}$	0.0	N
maximum robot pulling force	$F_{r,maxPull}$	0.0	N
maximum human pushing force	$F_{h,maxPush}$	98.1	N
maximum robot pushing force	$F_{r,maxPush}$	137.3	N
friction coefficient human	μ_h	1.1	
friction coefficient robot	μ_r	1.1	
object (box) mass	m	10.0	kg

perpendicular to the object face (Fig. 4), are assumed to be zero. Therefore, the maximum allowed tangential forces depend on the normal forces and the friction coefficients, i.e., $F_{maxT,i} = \mu_i |F_{N,i}|$, with the friction coefficients μ_i .

The parameter values used in the presented cases are listed in Table II. Since REBA considers a maximum load of 10 kg, this was set as the maximum allowed human pushing load. The robot arms have a maximum load specification of 14 kg. The friction coefficients are an estimate based on the friction coefficients of combinations of materials the human and robot hands and the box are made of.

As for the full-body poses, the loads are precomputed and stored in a table for fast retrieval during planning.

VII. EXPERIMENTAL RESULTS

The ergonomic planner is tested in a small user study of four people (1 female, 3 male), ranging in height between 1.70 and 1.95 m, on the task of collaboratively rotating the box 180°, clockwise and counterclockwise. The subjects were specifically chosen for their differences in size and build in order to prove the concept. The ergonomic performance of the planner is compared to that of the planner without the ergonomic cost term. In order to evaluate the quality of the ergonomic planner, the participants need to follow the robot’s collaborative plan for them. The plan is displayed on a large screen next to the robot.

The planner is evaluated in simulation and in an experimental setup with the robot depicted in Fig. 1. During the experiments, the participants wear an Xsens motion capture suit [28] to measure their poses. The REBA scores are computed from the predicted, respectively measured, poses combined with the estimated loads. Measurements of the robot hand forces show an average force estimation error of 0.4 N, with a standard deviation of 9.8 N. Compared the average predicted force of 25.9 N, this is accurate enough for our purposes.

Fig. 6 shows seven states out of a sequence proposed by the ergonomic (top row) and baseline (bottom row) planners for the goal of rotating the box 180°. The original planner just tries to minimize the time to task completion. As a result, the height of the object is held constant and, by default, the robot always regrasps first. For a fair comparison between the two planners, the height of the object in the initial state is the ergonomically optimal height of the starting pose according to the human pose model.

The ergonomic planner adjusts the height to optimize ergonomics. Who regrasps first also depends on what is most

TABLE III

PREDICTED AND MEASURED REBA SCORES OF THE ERGONOMIC AND BASELINE PLANNER FOR ROTATING A 10 kg OBJECT BY 180°, MEAN±STD FOR FOUR DIFFERENT PEOPLE AND TWO ROTATION TASKS EACH (CLOCKWISE AND COUNTERCLOCKWISE ROTATION).

		Average REBA	Maximum REBA	% of time with REBA ≥ 8
Planned	ergonomic planner	4.6±0.2	6.5±1.1	0.9±1.5
	baseline planner	6.0±0.7	7.8±0.4	25.2±24.2
Measured	ergonomic planner	5.1±1.2	7.9±0.9	5.9±6.3
	baseline planner	5.5±1.6	8.0±1.3	17.7±18.0

ergonomic for the human. This can be observed in states C and D in Fig. 6. The baseline planner requires the human to stay in a very unergonomic pose until the robot has regrasped twice, while the ergonomic planner allows the human to regrasp to a more ergonomic pose as quickly as possible and to stay in the more ergonomic pose as long as possible.

Figures 7 and 8 show the predicted, respectively the measured, REBA scores from the ergonomic and baseline planners. The dashed lines indicate the seven states corresponding to the snapshots in Fig. 6. Due to safety reasons, the robot takes 6.0 s for regrasping or rotating the object. Height adjustments can be performed much faster and when it is the human’s turn to regrasp, a 3.0 s transition time is much more comfortable for the human. With a longer transition time, the humans would need to take active care not to be too fast. This results in some state changes in the ergonomic planner occurring at a different time than in the baseline planner.

Fig. 7 shows lower REBA scores for the ergonomic planner whenever a more ergonomic alternative can be found. The results in Fig. 8 also generally show a REBA score below the score associated with the baseline planner. Up to about 35 s, the predicted REBA scores are reflected in the measurements, except for the ergonomic plan not actually getting the REBA score as low as 3. Around 30 s and in the last 7 s, the baseline plan was executed surprisingly ergonomically, resulting locally in a lower REBA score for the baseline planner.

The ergonomic plan differs from person to person, which indicates the planner accounts for subject-specific differences. Table III lists the combined results of the planners for all participants of the user study, each of whom rotates the box clockwise and counterclockwise, once in simulation and once together with the physical robot. Averaged over all generated plans, the predicted average REBA score is clearly lower for the ergonomic planner compared to the baseline planner, and the standard deviation is smaller. In a single case, the predicted maximum REBA score was as high for the ergonomic planner as for the baseline planner. This is the case when no more ergonomic alternative is known by the pose estimator. Except for one single case (state B in Fig. 6 and Fig. 7), the ergonomic planner could avoid plans including poses in the “High Risk” category, i.e., REBA ≥ 8 .

The REBA scores observed during the experiments show

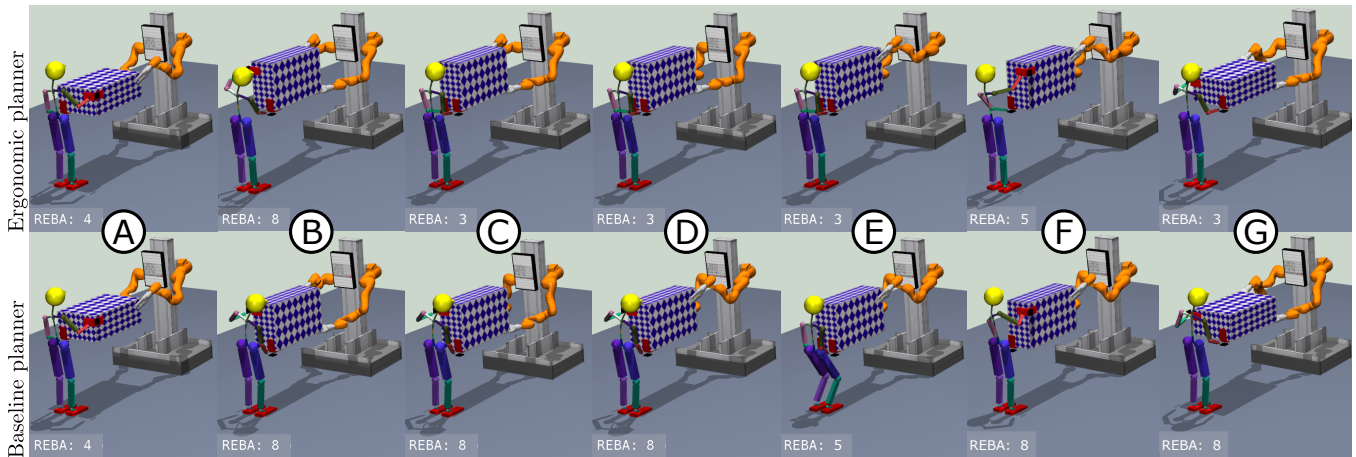


Fig. 6. Ergonomic planner (top) versus baseline planner (bottom) showing seven states of the planned sequence for rotating the box $+180^\circ$. At the bottom of each subfigure the REBA score is printed. The states correspond to the dashed lines in Fig. 7.

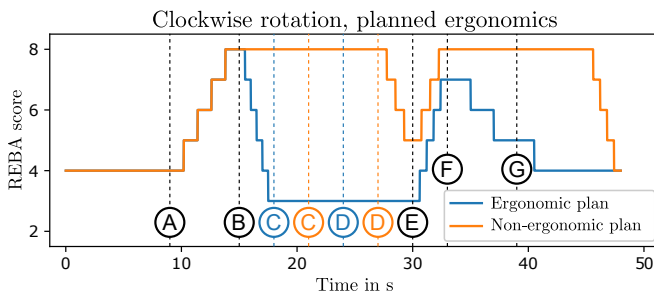


Fig. 7. Predicted ergonomic scores for the ergonomic and the baseline planner for rotating the box $+180^\circ$. The dashed lines correspond to the states depicted in Fig. 6 is reached. In case of states C and D the two planners differ in when the state is reached (see lines in corresponding colors).

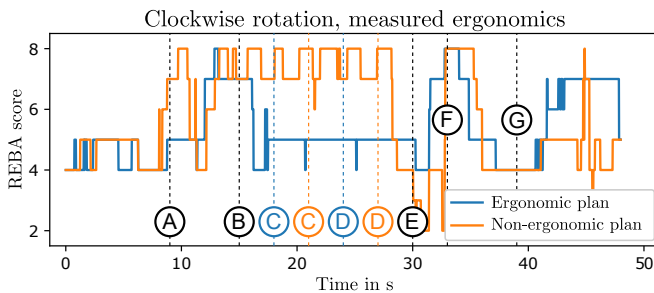


Fig. 8. Measured ergonomic scores for the ergonomic and the baseline planner for rotating the box $+180^\circ$. As in Fig. 7, the dashed lines correspond to the states depicted in Fig. 6.

smaller differences between the two planners. Though large differences were observed between participants, in general the ergonomic planner still yields a lower ergonomic cost, and the amount of time spent in poses with a ‘high’ ergonomic risk is reduced considerably. In all cases the standard deviation is lower for the ergonomic planner.

VIII. CONCLUSION AND DISCUSSION

This paper presents a novel concept for computing optimal ergonomics-enhanced plans in cooperative physical human-robot interaction tasks. The first contribution is a novel

human model which allows for prediction of an ergonomic assessment corresponding to a state within a task. It consists of a learned pose model and a computational load model. The pose model is trained with human motion capture data in order to predict the human pose as realistically as possible. The load model assumes some prior knowledge of the task, such as the mass and geometry of the manipulated object. Given a state within the task, the pose and load models provide the human pose and corresponding interaction forces for calculating a corresponding ergonomics score. Our prediction model gives a subject-specific estimate of the ergonomics of the states within a task.

The second contribution is the integration of this prediction model with a planning algorithm. The presented planner incorporates states and actions for both robot and human. This allows the computation of sequential plans optimized for human ergonomics. It is also possible to compute plans with a guaranteed upper bound on the permissible ergonomics score. We have shown in simulation and robot experiments of a collaborative human-robot box-rotating task that the proposed concepts lead to improved human ergonomics. Evaluation of the proposed ergonomics-enhanced planner in more complex collaborative tasks remains for future work.

In this paper, we selected the REBA score for ergonomic assessment. However, the system is flexible enough to allow for incorporating other ergonomics indicators. For future use of the proposed method, exploration into the effects of incorporating alternate ergonomics indicators is recommended, as the discrete nature of REBA sometimes causes a large difference in ergonomic cost for very small posture changes.

This paper demonstrates our approach to be capable of finding a plan which affords improved ergonomics for people working with a robot. Future work will focus on concepts to encourage the human to follow the ergonomic plan, and reacting appropriately when the human does not.

ACKNOWLEDGMENT

The authors thank Dirk Ruiken for his kind support.

REFERENCES

- [1] V. Villani, F. Pini, F. Leali, and C. Secchi, "Survey on human-robot collaboration in industrial settings: Safety, intuitive interfaces and applications," *Mechatronics*, vol. 55, pp. 248–266, 2018.
- [2] B. R. da Costa and E. R. Vieira, "Risk factors for work-related musculoskeletal disorders: a systematic review of recent longitudinal studies," *American J. Industrial Medicine*, vol. 53, no. 3, pp. 285–323, 2010.
- [3] Siemens PLM Software. (2019) Jack. [Online]. Available: <https://www.plm.automation.siemens.com/store/en-us/jack/>
- [4] P. Maurice, V. Padois, Y. Measson, and P. Bidaud, "Human-oriented design of collaborative robots," *Int. J. Industrial Ergonomics*, vol. 57, pp. 88–102, 2017.
- [5] M. Gienger, D. Ruiken, T. Bates, M. Regaieg, M. Meißner, J. Kober, P. Seiwald, and A.-C. Hildebrandt, "Human-robot cooperative object manipulation with contact changes," in *IEEE/RSJ Int. Conf. Intelligent Robots and Systems (IROS)*, 2018.
- [6] B. Nemeč, N. Likar, A. Gams, and A. Ude, "Human robot cooperation with compliance adaptation along the motion trajectory," *Auton. Robots*, vol. 42, no. 5, pp. 1023–1035, 2018.
- [7] F. Ficuciello, L. Villani, and B. Siciliano, "Variable impedance control of redundant manipulators for intuitive human-robot physical interaction," *IEEE Trans. Robotics*, vol. 31, no. 4, pp. 850–863, 2015.
- [8] L. Roveda, S. Haghshenas, M. Caimmi, N. Pedrocchi, and L. Molinari Tosatti, "Assisting operators in heavy industrial tasks: on the design of an optimized cooperative impedance fuzzy-controller with embedded safety rules," *Frontiers Robotics and AI*, vol. 6, p. 75, 2019.
- [9] D. J. Agravante, A. Cherubini, A. Sherikov, P.-B. Wieber, and A. Kheddar, "Human-humanoid collaborative carrying," *IEEE Trans. Robotics*, vol. 35, no. 4, pp. 833–846, 2019.
- [10] E. Gribovskaya, A. Kheddar, and A. Billard, "Motion learning and adaptive impedance for robot control during physical interaction with humans," in *IEEE Int. Conf. Robotics and Automation (ICRA)*, 2011.
- [11] J. DelPreto and D. Rus, "Sharing the load: Human-robot team lifting using muscle activity," in *IEEE Int. Conf. Robotics and Automation (ICRA)*, 2019.
- [12] L. Peternel, N. Tsagarakis, and A. Ajoudani, "Towards multi-modal intention interfaces for human-robot co-manipulation," in *IEEE/RSJ Int. Conf. Intelligent Robots and Systems (IROS)*, 2016.
- [13] J. Bütepage, H. Kjellström, and D. Kragic, "Anticipating many futures: Online human motion prediction and synthesis for human-robot collaboration," in *IEEE Int. Conf. Robotics and Automation (ICRA)*, 2018.
- [14] G. Maeda, M. Ewerton, G. Neumann, R. Lioutikov, and J. Peters, "Phase estimation for fast action recognition and trajectory generation in human-robot collaboration," *Int. J. Robotics Research*, vol. 36, no. 13-14, pp. 1579–1594, 2017.
- [15] K. P. Hawkins, S. Bansal, N. N. Vo, and A. F. Bobick, "Anticipating human actions for collaboration in the presence of task and sensor uncertainty," in *IEEE Int. Conf. Robotics and Automation (ICRA)*, 2014.
- [16] T. Stouraitis, I. Chatzinikolaïdis, M. Gienger, and S. Vijayakumar, "Dyadic collaborative manipulation through hybrid trajectory optimization," in *2nd Conf. Robot Learning*, 2018.
- [17] W. Kim, J. Lee, L. Peternel, N. Tsagarakis, and A. Ajoudani, "Anticipatory robot assistance for the prevention of human static joint overloading in human-robot collaboration," *IEEE Robotics and Automation Lett.*, vol. 3, no. 1, pp. 68–75, 2018.
- [18] L. Peternel, W. Kim, J. Babič, and A. Ajoudani, "Towards ergonomic control of human-robot co-manipulation and handover," in *IEEE-RAS 17th Int. Conf. Humanoid Robotics (Humanoids)*, 2017.
- [19] A. G. Marin, M. S. Shourijeh, P. E. Galibarov, M. Damsgaard, L. Fritzsche, and F. Stulp, "Optimizing contextual ergonomics models in human-robot interaction," in *IEEE/RSJ Int. Conf. Intelligent Robots and Systems (IROS)*, 2018.
- [20] A. Shafti, A. Ataka, B. U. Lazpita, A. Shiva, H. A. Wurdemann, and K. Althoefer, "Real-time robot-assisted ergonomics," in *IEEE Int. Conf. Robotics and Automation (ICRA)*, 2019.
- [21] L. McAtamney and E. N. Corlett, "RULA: A survey method for the investigation of work-related upper limb disorders," *Applied Ergonomics*, vol. 24, no. 2, pp. 91–99, 1993.
- [22] B. Busch, M. Toussaint, and M. Lopes, "Planning ergonomic sequences of actions in human-robot interaction," in *IEEE Int. Conf. Robotics and Automation (ICRA)*, 2018.
- [23] AnyBody Technology A/S. [Online]. Available: www.anybodytech.com
- [24] G. David, "Ergonomic methods for assessing exposure to risk factors for work-related musculoskeletal disorders," *Occupational Medicine*, vol. 55, no. 3, pp. 190–199, 2005.
- [25] S. Hignett and L. McAtamney, "Rapid entire body assessment (REBA)," *Applied Ergonomics*, vol. 31, no. 201, p. 205, 2000.
- [26] S. Vijayakumar and S. Schaal, "Locally weighted projection regression: An $O(n)$ algorithm for incremental real time learning in high dimensional space," in *17th Int. Conf. Machine Learning (ICML)*, 2000.
- [27] M. Gienger, H. Janssen, and C. Goerick, "Task-oriented whole body motion for humanoid robots," in *5th IEEE-RAS Int. Conf. Humanoid Robots*, 2005.
- [28] D. Roetenberg, H. Luinge, and P. Slycke, "Xsens MVN: full 6dof human motion tracking using miniature inertial sensors," Xsens Motion Technologies BV, Tech. Rep., 2009.